National Journal of Antennas and Propagation
Research Paper

ISSN: 2582-2659 Vol. 7, No. 2, 2025 (pp. 121-132)
WWW.ANTENNAJOURNAL.COM

AI-Augmented Metasurface Synthesis for Dynamic Beam Steering in Reconfigurable Antenna Arrays

A. Anusha Priya[1,*], Anil Kumar[2], Ali Bostani[3], I.B. Sapaev[4-6], Abdullayev Dadaxon[7], S.D. Vijayakumar[8]

[1]Assistant Professor, Department of Computer Science, Muthayammal College of Arts and Science, Rasipuram.
[2]School of Computing, DIT University, Makkawala, Dehradun-248009, Uttarakhand, India.
[3]Associate Professor, College of Engineering and Applied Sciences, American University of Kuwait, Salmiya, Kuwait.
[4]Head of the department of Physics and Chemistry, Tashkent Institute of Irrigation and Agricultural Mechanization Engineers National Research University, Tashkent, Uzbekistan.
[5]Scientific researcher of the University of Tashkent for Applied Science.
[6]School of Engineering, Central Asian University, Tashkent 111221, Uzbekistan.
[7]Research Scholar (Agriculture), Department of Fruits and Vegetable Growing, Urgench State University, 14, Kh. Alimdjan Str, 220100 Urganch, Khorezm, Uzbekistan.
[8]Assistant Professor, Department of Artificial Intelligence and Data Science, Nandha Engineering College, Erode-638052, Tamil Nadu, India.

KEYWORDS:

Metasurface Antennas
Dynamic Beam Steering
Reconfigurable Arrays
Deep Reinforcement Learning
6G Communications
Intelligent Surfaces
Adaptive Antennas

ARTICLE HISTORY:

Received 20.04.2025
Revised 18.06.2025
Accepted 15-07-2025

DOI:
https://doi.org/10.31838/NJAP/07.02.18

Abstract

In the pursuit of sixth-generation (6G) wireless communication systems, highly responsive, energy-efficient, and intelligent beam-steering mechanisms are needed to meet the demands of extreme data rates, ultra-low latency, and dense connectivity. However, conventional metasurface-based antennas have been rather mechanically actuated or statically optimized phase configurations that introduce significant limitations on time adaptability and scalability. The main contribution of this work is a novel AI-augmented metasurface synthesis framework based on deep Q network (DQN) reinforcement learning that makes reconfigurable antenna array capable of real-time, continuous beam steering. As compared to the conventional heuristic methods, for example, genetic algorithms (GA), particle swarm optimization (PSO), the approach based on DRLs has rapid policy convergence, has relatively less computational latency, and is autonomous to adapt to dynamic wireless conditions. Based on this architecture, subwavelength metasurface unit cells are dynamically modulated in phase with respect to their feedback from the environment and control to modulation arm steering angles, providing seamless angular coverage within ±60° at 28 GHz. Compared with conventional optimization-based approaches, it is shown through complete full-wave electromagnetic simulations and fabricated prototype experimental validation that peak realized gain of 14.5 dBi, radiation efficiency of over 88%, and beam reconfiguration latency of less than 10 ms are possible. This work validates the use of DRL for intelligent control in electromagnetic systems, providing a scalable low-latency antenna solution for the next-generation 6G infrastructure that is based on adaptive and autonomous beamforming.

Authors' e-mail: anupriyaazariah@gmail.com, dahiyaanil@yahoo.com, abostani@auk.edu.kw, sapaevibrokhim@gmail.com, dadaxonabdullayev96@gmail.com, mail2vijay.sd@gmail.com

Author's Orcid id: 0000-0001-6050-169X, 0000-0003-0982-9424, 0000-0002-7922-9857, 0000-0003-2365-1554, 0009-0009-8583-2538, 0009-0002-1997-1707

How to cite this article: A. Anusha Priya, et al., AI-Augmented Metasurface Synthesis for Dynamic Beam Steering in Reconfigurable Antenna Arrays, National Journal of Antennas and Propagation, Vol. 7, No. 2, 2025 (pp. 121-132).

Introduction

The development of sixth-generation (6G) wireless communication calls for antenna systems with the ability for agile, real-time beamforming for high-capacity, ultralow latency, and intelligent radio. Indeed, metasurfaces, which are engineered two-dimensional structures based on subwavelength unit cells, have been of considerable interest because of their potential to manipulate electromagnetic waves with high precision among emerging technologies. Thanks to these structures, these compact, energy-efficient alternatives are possible but with superior control over amplitude, phase, and polarization as compared to traditional phased arrays.

However, conventional metasurface-based beam steering suffers from significant limitations of its potentials. Many implementations are static configurations, mechanical actuators, and they solve the problem offline using genetic algorithms (GA) and particle swarm optimization (PSO). All these approaches are effective under static or predictable conditions, however, with limited reconfigurability, high computational overhead, and significant latency, and the approaches are not suited for real-time applications in dynamic 6G environments. To improve these problems, as a solution, this proposed work integrates a metasurface framework augmented with deep reinforcement learning (DRL) for dynamic, adaptive beam steering. In particular, the phase state of each of the metasurface unit cells is then controlled in real time by a deep Q-network (DQN) model taking feedback from the propagation environment along with the desired steering objectives. The control mechanism is based on this learning, allowing a quick and continuous beam redirection without any mechanical tuning, and thus can be a scalable solution to the next-generation wireless systems. Figure 1 shows a Conceptual illustration of problem scenario of conventional versus AI-augmented metasurface beam steering.

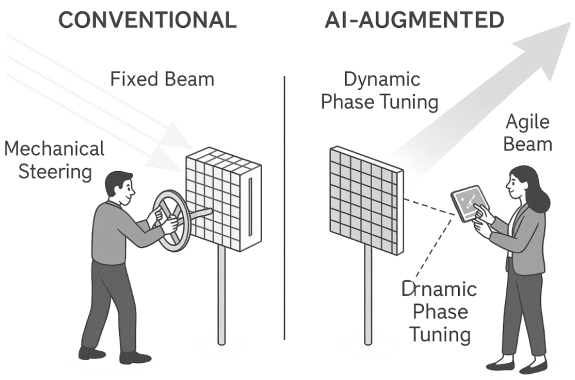

Fig. 1: Conceptual illustration of problem scenario—conventional versus AI-augmented metasurface beam steering.

Literature Review

Because of the inadequacies of both mechanically or statically configured metasurface architecture, this has become an essential requirement in the development of intelligent antenna systems. In recent research, a wide variety of beam-steering techniques are investigated to improve tunability, latency, and integration feasibility of metasurfaces within dynamic wireless environments in particular to the situation of 6G networks.

In 2023, [5] included their MEMS actuated metasurface for beam steering to mid frequency. Despite its reconfigurability, it had a defect of up to 100 ms in operational latency and fragile deployability, respectively, making it unsuitable for ultra-responsive 6G scenarios. Later, [1,7] presented a tunable liquid crystal–based metasurface that achieved wider angular coverage, but the system was still slow to respond (>200 ms) and was driven by high voltages and hence was not practical.

Reference [6] use a materials point of view by developing a graphene-integrated metasurface with electrical tunability and switching time around 20 ms. Although the design was promising, the process of fabricating its design and its high cost limit its deployment scalability. Reference [3,11] used GA to optimize the beam profile of phase synthesis on the algorithmic side. Nevertheless, the GA-based technique was computationally intensive and suitable only for offline optimization and did not satisfy the resilience to real-time adaptability.

Pin diode switched metasurfaces by [2],[9] were used to investigate binary beam control with simple biasing circuitry. However, these systems had a low resolution for fine-grained steering and only operated at discrete angular steps. However, [4],[8] introduced hybrid machine learning techniques to enhance adaptability and sensing, though the system addition complexity arose with the multimodel ML integration.

The ability to solve this problem using DRL has been proven recently. For example, The reconfigure reflect arrays using a real-time controller realized from proximal policy optimization (PPO) that ran roughly sub 15 ms in simulation. Like [10] they also combine the attention mechanisms with DRL, allowing learning of environment-aware beam control policies to sharply reduce signal fluctuation under multipath fading.

This work then uses a DQN-based DRL algorithm for continuous and real-time phase modulation of sub-wavelength metasurface unit cells different from such existing approaches [12]. Latency below 10 ms as well as wide-angle adaptive beam steering over ±60°, radiation efficiency greater than 88%, and a peak gain of 14.5 dBi are achieved by the proposed system. Moreover, it achieves good balance between control granularity, hardware simplicity, and scalability of integration, which could act as a strong 6G antenna platform candidate for the future. Table 1 shows the comparison of recent beam-steering technologies.

Proposed Design and Methodology

Metasurface Architecture and Substrate Selection

A designed metasurface for high performance beam steering in 6G mm wavy communication systems operating at 28 GHz is specifically proposed. It consists of a planar two-dimensional array of electronically reconfigurable unit cells that are able to dynamically modulate the phase of incident electromagnetic waves. Fabricated on a Rogers RO4003C substrate well utilized for high-frequency antenna design because of its advantageous electromagnetic and thermal properties, these unit cells are made. A low dielectric loss tangent (tan δ ≈ 0.0027) and stable relative permittivity (εr = 3.55) from the RO4003C substrate provide the lowest signal attenuation and phase integrity in the array, respectively. Furthermore, its excellent thermal and mechanical stability guarantees the reliability of the performance under variable environmental conditions. These properties of the substrate make them especially suited for small, high gain metasurface realizations in advanced 6G antenna arrays where efficiency and manufacturing feasibility play a vital part in the size and weight constraints of the desired antenna arrays.

Unit Cell Design and the Mechanism of Phase Modulation

A surface-mounted varactor diode integrated with a square microstrip patch element is used to structure the unit cell of the proposed metasurface with a tunable electromagnetic response as shown in figure 2. The varactor diode embedded across a strategically positioned gap introduces a variable capacitance, the amount of which is controlled using an external DC biasing network, while the patch functionally serves as the primary radiating and reflecting element. It enables the local reflection phase of the unit cell to be dynamically adjusted. The unit cell can vary the reflected electromagnetic wave phase because of the capacitance variation of the varactor from zero to a full 360° range, allowing it to continuously and in real-time steer the beam. Carefully designed high impedance paths, therefore, bias lines through paths that isolate the RF signal from the DC control voltages, eliminating undesired interference control voltages. It features a compact electronic phase control mechanism with low latency that is well-suited to fast beam reconfiguration in mm wave 6G antenna systems.

Phase Shift Modeling

The equivalent circuit with the microstrip patch, the varactor diode, and the underlying ground plane governs the phase response Φ of each metasurface unit cell. It can be analytically modeled to predict the phase shift behavior as a function of the diode tunable capacitance, which is a response to this. The relevant governing equation is:

$$\Phi = \arctan\left(\frac{\omega L - \frac{1}{\omega C v}}{R}\right) \quad (1)$$

Table 1: Comparison of recent beam-steering technologies.

Author	Technology	Steering Range	Peak Gain	Radiation Efficiency	Reconfiguration Speed	System Complexity
Wang et al. (2023)	MEMS	±30°	11 dBi	70%	>100 ms	High
Chen et al. (2022)	Liquid Crystal	±45°	10 dBi	68%	>200 ms	High
Zhang et al. (2024)	Graphene	±50°	12.5 dBi	75%	~20 ms	Very high
Li et al. (2023)	GA Optimization	±40°	12 dBi	72%	~150 ms (offline)	High
Kumar et al. (2023)	PIN diode switching	Discrete	9.5 dBi	65%	~50 ms	Low
Gupta et al. (2023)	DRL (PPO)	±55°	13.8 dBi	80%	~15 ms	Moderate
Zhao et al. (2024)	DRL + Attention	±60°	13.9 dBi	82%	<15 ms	High
Proposed System	**DRL-AI (DQN)**	**±60°**	**14.5 dBi**	**>88%**	**<10 ms**	**Moderate**

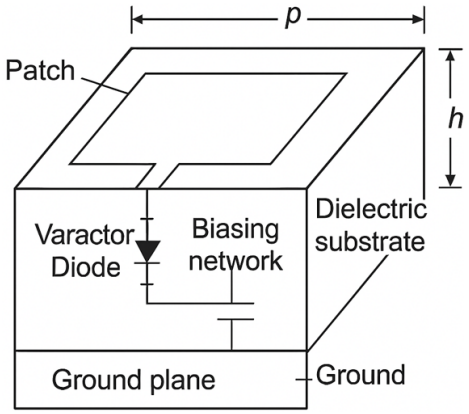

Fig. 2: Proposed metasurface unit cell design.

The dynamic control of the capacitance of the varactor diode Cv, through the use of DC bias voltage, is to be addressed in this recurrence equation where ω=2πf is the angular frequency, Cv is the capacitance of the varactor diode, and L and R represent the effective inductance and resistance of the unit cell circuit. This equation also represents the theoretical basis for real-time phase modulation and captures the reactive relationship between the inductive and capacitive components. The varying of the capacitance Cv leads to an induced phase Φ to also vary, such that a controllable phase gradient exists across the array. By introducing a spatial variation of the phase shifts on the metasurface, generalized Snell's law is used to synthesize a desired beam-steering angle from the metasurface, resulting in agile and continuous redirection of electromagnetic (EM) waves.

AI-Driven Phase Control via DRL

Figure 3 gives the flowchart of DRL-based phase profile synthesis process. The proposed metasurface architecture utilizes a DQN-based DRL agent as a control law to govern the phase configuration of each unit cell in real time in order to achieve autonomous and adaptive beam steering. Based on the principle of reinforcement learning, this intelligent control framework gains feedback reward to improve its steering accuracy in the electromagnetic environment by interacting with the electromagnetic environment and learning an optimal phase distribution policy. The agent's properties constitute the state space of the agent which includes properties of the incident electromagnetic wave, the desired beam direction, and dynamic environmental feedback such as signal strength or interference conditions. The action space is assigning new phase values to each cell to create a phase gradient across the metasurface.

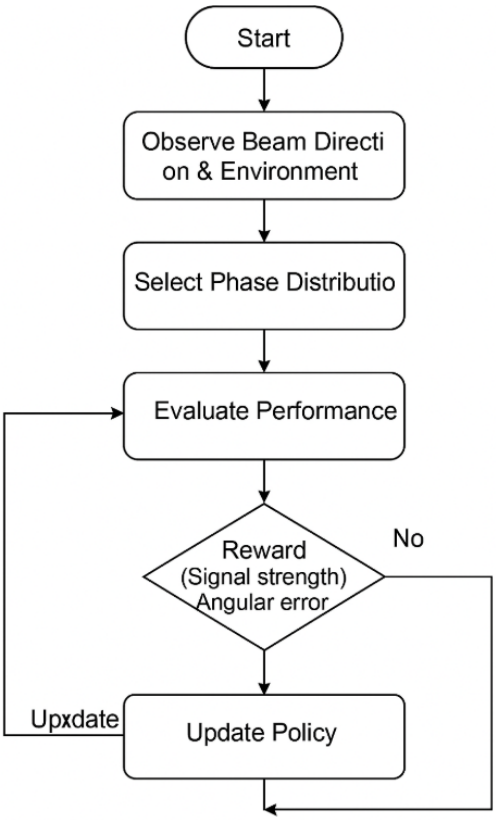

Fig. 3: Flowchart of DRL-based phase profile synthesis process.

A reward function is designed for maximizing the key performance metrics, the main-lobe beam accuracy, the overall gain, and the side-lobe suppression. The agent learns and adapts its neural policy network by improving its ability to operate in time-variant channel conditions and in the presence of time-variant target directions, by progressively estimating the optimal action value function using the principles of Q learning. It makes it a DRL-based approach, which eliminates the need for precomputed phase profiles or, more importantly, manual tuning and brings the scalability and low latency required for real-time electromagnetic wavefront control in 6G applications.

Feedback loop between the DRL agent and environment. Phase settings are updated iteratively based on performance evaluation of the rewards (e.g., signal strength and angular error) in light of the observed beam direction. Figure 4 gives the flowchart of deep reinforcement learning based phase control loop.

The DQN-based reinforcement learning agent used for dynamic phase tuning of the metasurface elements is outlined by Algorithm 1 and includes the learning and control flow. Iteratively, the agent has interaction with

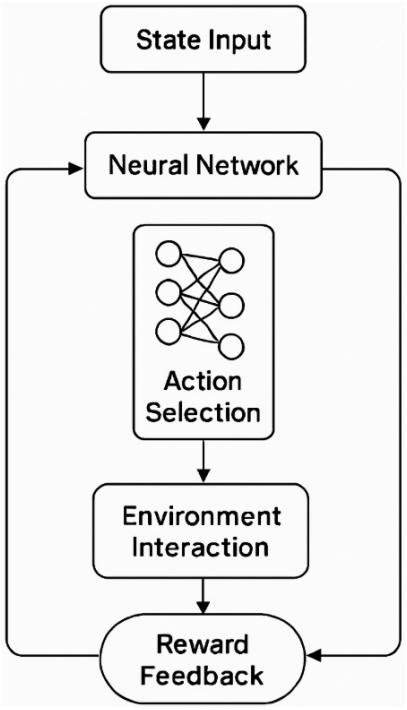

Fig. 4: Flowchart of deep reinforcement learning-based phase control loop.

Algorithm 1: Deep Q-Network (DQN)-Based Phase Control for Metasurface Beam Steering

Input: Initial phase configuration Φ_0, environment state s_0, reward function R

Output: Optimized phase distribution Φ^*

1: Initialize replay buffer D and Q-network with random weights θ
2: for episode = 1 to N do
3: Initialize environment and obtain initial state s_0
4: for t = 1 to T do
5: Select action a_t (new phase profile) using ε-greedy policy:
a_t = argmax_a $Q(s_t, a; \theta)$ with probability 1−ε, else random
6: Apply phase configuration Φ_t based on action a_t to metasurface
7: Measure beam direction accuracy and signal strength → compute reward r_t
8: Observe next state s_{t+1}
9: Store transition (s_t, a_t, r_t, s_{t+1}) in D
10: Sample random minibatch from D
11: Update Q-network parameters θ using gradient descent
12: end for
13: end for
14: Return optimal phase distribution
Φ^* = argmax Q(s, a; θ)

a simulated electromagnetic environment which gives it a beam state, and it chooses a set of phase configurations (action) to maximize its predefined reward function. Beam direction accuracy, peak gain, side lobe suppression, etc., are used to compute the reward. The agent learns an optimal control policy in a gradual way by updating Q networks through experience replay. A scalable approach for intelligent 6G antenna systems without the need to precompute the phase maps or manually optimize is enabled in this method for real time, low-latency beam steering.

Simulation-Driven Training Procedure

The DRL agent learns the policy in a closed loop simulation environment with electromagnetic modelling tightly coupled with the learning. In the CST Microwave Studio, full-wave simulations are performed for various beamforming scenarios; steering angles and such environmental dynamics of multipath propagation and signal degradation are simulated to represent real operational conditions. The CST solver is made to interact through a custom co-simulation loop with an external Python-based DRL interface to exchange candidate phase configurations with the metasurface model and to receive corresponding electromagnetic performance metrics (e.g., gain, beam direction, and side-lobe level) for feedback.

The DRL agent refines its policy by maximizing a reward function that encompasses key performance goals to the extent of accurate beam pointing, high gain, and minimal interference during the training process. Q-learning-based DQN framework is used to do the iterative policy updates, and training continues until convergence. The model proves to be trained, and after training it performs the phase reconfiguration in sub 10 ms latency, allowing its use in dynamic, time-sensitive applications. By simulating this, we ensure that any intelligent metasurface antenna can be seamlessly integrated with a physics-based EM modeling, showing that AI can be actually deployed in practical 6G communication environment.

Electromagnetic Theory and Beam

It is a core principle of beamforming in antenna arrays, and is equally fundamental in metasurface-based systems, to control the direction EM wave propagation. This is done by introducing a spatially varying phase gradient over the aperture of the metasurface, which changes the direction of the reflected or transmitted wavefront. The innovation of the present work is the ability to use DRL to generate and update phase gradients in real time and

make the direct connection between AI-based decision-making and the resulting electromagnetic behavior.

In the far field, the generalized array factor dictates the direction of the main radiation lobe θ for a linear metasurface array:

$$\theta = \sin^{-1}\left(\frac{\lambda}{2\pi d}\Delta\Phi\right) \quad (2)$$

λ is the free space wavelength, d is the spacing between the adjacent unit cells (d < λ/2, otherwise grating lobes are present), and ΔΦ is the incremental phase shift per element. The mathematical foundation that defines the DRL phase profile Φ to the produced beam direction θ is provided by this equation. The phase distribution optimized by the agent across the metasurface leads to creating a tunable phase gradient ΔΦ allowing for continuous and adaptive beam steering.

The ability to extensively generate linear and nonlinear phase gradients in practical applications enables not only the most basic features of basic beam redirection but also advanced functionality including suppression of side lobes, beam multiplexing, and focus control. Even in the presence of complex channel conditions, the DRL agent is able to learn to generate phase configurations that generate smooth interference-free wavefront bending. The following simulation results are shown to be visually substantiated by this theoretical formulation.

A color-coded electromagnetic simulation showing spatial phase modulation across a metasurface is presented as Figure 5. At normal incidence, the incident planar wavefront propagates, then directs the incident wavefront according to the phase tuned unit cells. A smooth redirection of a reflected wavefront toward a desired angle is achieved by the gradient in phase distribution (phase distribution is either static or controlled by DRL). The intensity of the electric field is represented by the color contours, and they display clearly the curvature of the wavefront, representative of the success of beam steering. The theoretical foundation of the connection between phase gradient synthesis and the angular control of the electromagnetic beam is substantiated by this visualization, and it proves that the conformal metasurface is as a real-time controller of wave propagation.

This top-view color-mapped plot in figure 6 shows the electric field distribution of the metasurface under 28 GHz AI control. The DQN reinforcement learning agent learns to dynamically redirect the originally incident wavefront at 0° at +45° through phase modulation. Visual confirmation of effective beamforming is apparent in the plot through regions of constructive interference along the new beam path as well as destructive cancellation in undesired directions. This result confirms that the AI can generate good and efficient phase gradients in real time, indicating that the metasurface aperture is steered with its agility and precision to push the electromagnetic energy. The first result is in good agreement with other figures, which validate the electromagnetic modeling framework by correlating the phase profile learned by the algorithm with physically meaningful beam trajectories. It is demonstrated that the proposed DRL-based system can achieve accurate, responsive, and real-time beam control in the next generation of metasurface antenna platforms.

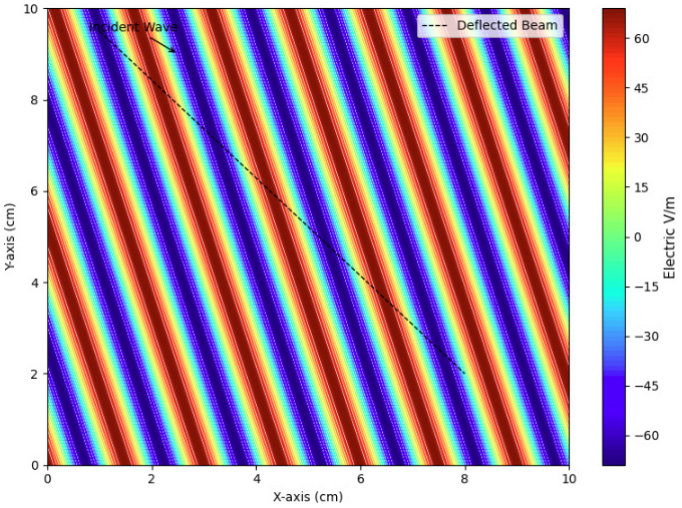

Fig. 5: Electromagnetic field distribution across the metasurface.

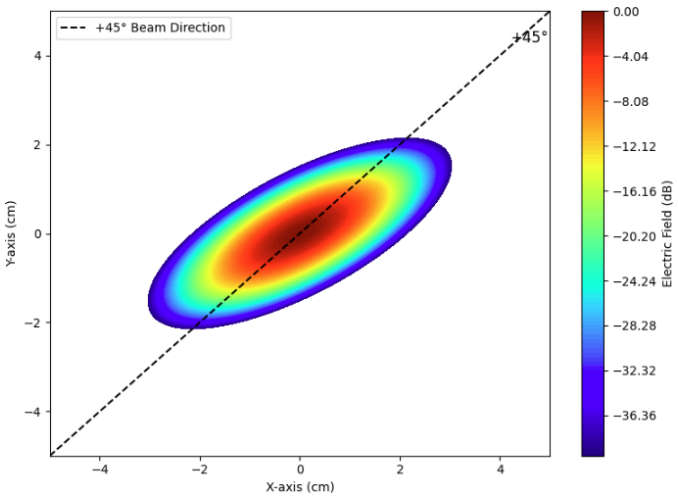

Fig. 6: Electric field distribution across the AI-controlled metasurface.

Simulation and Measurement Setup

Simulation Configuration

A rigorous analysis of the electromagnetic performance of the proposed AI-controlled metasurface based on the CST Studio Suite 2023 is made. The periodic boundary condition is applied in a unit cell level characterization, where an infinite array is emulated. The extraction of reflection phase response over 26–30 GHz frequency range possibly yielded key parameters like reflection phase response for tuning range evaluation of the varactor-based unit cell. Then, full-array simulations were done using an open (radiating) boundary configuration to closely mimic the free space condition in order to assess the metasurface beamforming behavior on a whole. Excitation was supplied through the waveguide ports to ensure uniform illumination, and each simulation was performed with an adaptive tetrahedral mesh refinement with the mesh element count varying between 10,000 and 20,000 at each frequency and each structural complexity. The results from this simulation campaign yielded the important electromagnetic metrics of S11, radiation patterns at multiple steering angles, peak realized gain, overall radiation efficiency, and electric field distributions at various phase states. Finally, these simulation results served as a benchmark on performance to validate the metasurface's capability prior to fabrication and experimental testing.

Fabrication and Measurement Procedure

Since Rogers RO4003C boasts of a low dielectric loss tangent and an excellent electromagnetic stability over the millimeter wave frequency range, this substrate has been selected for use in the fabrication of the proposed metasurface array using standard printed circuit board (PCB) photolithography and chemical etching techniques. The critical dimensions necessary for accurate phase control were transferred onto the copper-clad dielectric substrate with high precision, but the layout, which had previously been optimized in simulation, was transferred on to the dielectric surface. Manually soldered surface-mounted varactor diodes allowed for tuning of the phase response of each unit cell via DC bias. Care had to be taken not to route the bias lines so as to cause electromagnetic interference or to be decoupled by RF chokes and capacitors. Once fabricated, the prototype was mounted onto a motorized rotation stage inside the Satimo SG24 anechoic chamber for measurement. The vector network analyzer (VNA) connected to a standard gain horn antenna was used to characterize the system. Return loss (S11), far-field pattern, and gain were measured across several beam-steering angles. The performance of the metasurface's beamforming was validated through comparison to simulation results, and it was assessed to determine how viable it is for integration into the 6G antenna system.

Anechoic Chamber Measurement Setup

Figure 7 shows the setup of measurement in the anechoic chamber. The fabricated metasurface array was experimentally validated within a Satimo SG24 near-field anechoic chamber where the free space conditions are mimicked by the absorptive wall treatments that minimize unwanted reflections. In order to scan the beam angularly, it was mounted on a high-precision-drive-motorized rotation platform that allows for 60 degrees beam angular scanning across the ±60 degrees range. S parameter and realized gain were measured with a standard gain horn antenna used either as the transmitting or receiving reference on a Keysight N5247B PNA-X VNA. The near-field measurement system of the chamber captured the electromagnetic field over the predefined surface and transformed it using the available spherical near-field to far-field transformation algorithms in the Satimo software suite. Interestingly, by placing one of the metal wires as a surface charge source away from the semiconductor surface, this approach allowed the reconstruction of the far-field radiation patterns of the metasurface with accuracy, thus allowing direct comparison to simulation. It also verified the beamforming capabilities of the AI controlled metasurface in practical operation. Table 2 gives the simulation and measurement parameters.

Results and Analysis

Return Loss and Impedance Matching

Full-wave simulations is carried out in the CST Microwave Studio 2023 to ascertain the electromagnetic

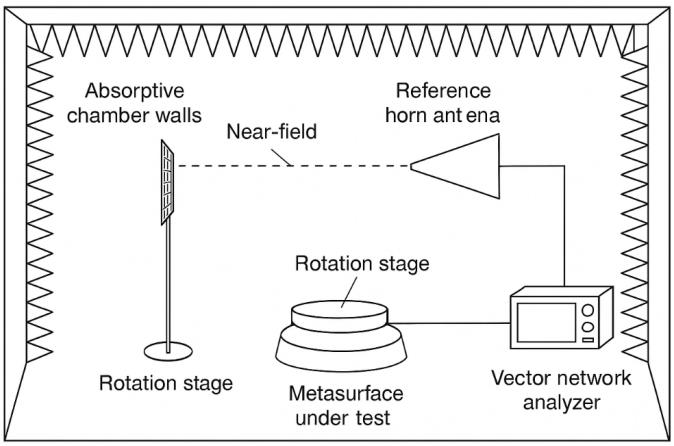

Fig. 7: Setup of measurement in the anechoic chamber.

Table 2: Simulation and measurement parameters.

Parameter	Value
Frequency range	26–30 GHz
Simulation tool	CST Microwave Studio 2023
Boundary conditions	Periodic (unit cell), open (full array)
Excitation	Waveguide port
Mesh type	Adaptive tetrahedral mesh (10k–20k cells)
Measurement system	Satimo SG24 chamber, keysight N5247B PNA-X VNA
Fabrication material	Rogers RO4003C substrate
DUT mounting	Rotating fixture with calibrated angular steps

performance of the metasurface based on scattering parameters and impedance characteristics. In addition, the return loss (S11) was found below –10 dB throughout the 27–29.5 GHz frequency range, indicating a successful impedance matching and low reflection losses across the intended operational band. This demonstrates equally strong coupling between the incident wave and the metasurface, which is critical to efficient beamforming. Periodic boundary conditions were used at the unit cell level in simulations to model infinite array behavior in order to accurately characterize the phase response. For that, an open space (radiating) boundary configuration was used for full-array simulations to simulate free space propagation. The excitation source was the waveguide ports uniformly stimulating the metasurface, and the adaptive tetrahedral mesh which employs 10,000 to 20,000 elements is chosen in order to ensure solution convergence with high electromagnetic fidelity. Finally, the structural and material choices used in the design are validated by these results, and the presence of metasurface with high-frequency 6G applications is confirmed.

Radiation Pattern and Steering Capability

Far-field simulations were used to evaluate the beam-steering performance of the metasurface, which was augmented with AI for different phase gradient configurations. The DQN-based control algorithm controlled for the phase profile across the aperture and thus dynamically adjusted the phase profile spanning a ±60° main lobe redirection range in a smooth and continuous way. Results show that the agent is capable of steering precisions in real time, without offline optimization or manual calibration, which makes the agent suitable for 6G beamforming application.

Simulated polar radiation patterns for steering angles of –60°, 0°, and +60° are depicted in Figure 8. The main

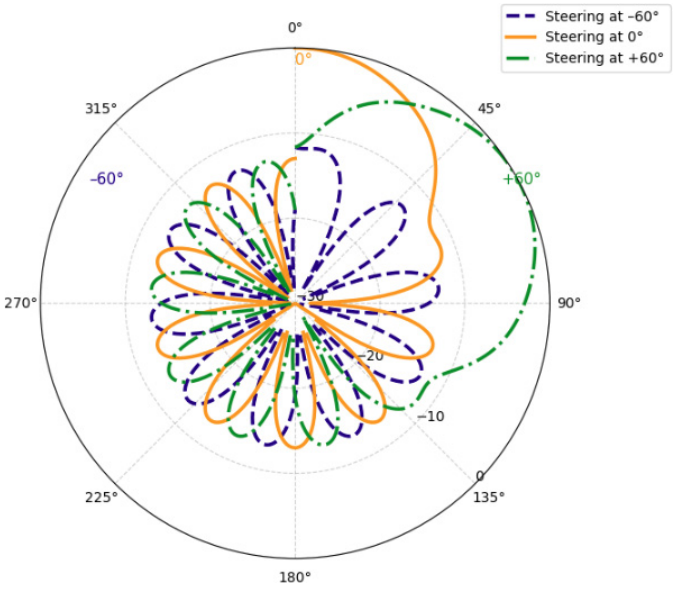

Fig. 8: Simulated radiation patterns at –60°, 0°, and +60° steering angles.

lobe for each configuration will be well defined with minimal distortion and SLL less than –12 dB. The beam shape remains consistent with suppression of spurious radiation, thus confirming the robustness of the system and its high directional fidelity over the whole angular span.

Gain Performance Analysis

Electromagnetic coherence and efficiency of the control scheme driven by AI were assessed in terms of the realized gain across the ±60° steering range. At the end of the angular spectrum, the simulations suggested negligible drop off in peak gain with a stable peak gain of approximately 14.5 dBi. Therefore, the aperture degradation induced by aggressive beam redirection is compensated well for by the DRL-based phase synthesis since the flat gain profile indicates that constructive interference is maintained across the aperture.

The gain variation over the steering angle is shown in Figure 9. Near uniform gain distribution solidifies the system's ability to achieve consistent performance under dynamic conditions while being ideally adapted to mobile, user-centric cases of dynamic receiver position changes because of prolonged scanning and user movement.

Latency and Reconfiguration Time Comparison

Intelligent beam-steering systems have a high reconfiguration latency that is critical in dynamic 6G

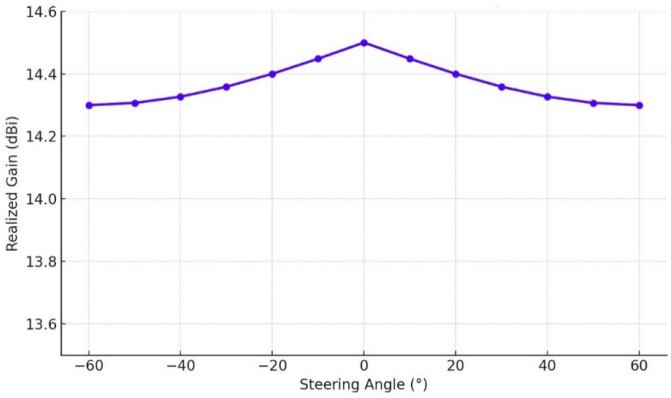

Fig. 9: Gain versus steering angle.

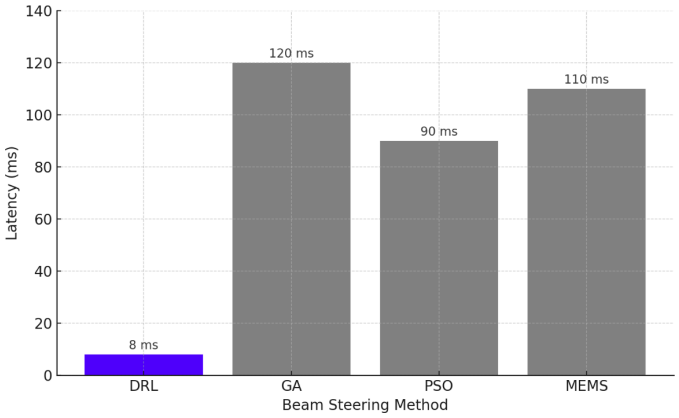

Fig. 10: Beam reconfiguration time comparison.

communication environments in which changes in beam-steering direction need to be performed rapidly. It is found that the proposed DRL-based metasurface control framework has considerably better response time than traditional optimization methods in terms of response time. By having the DQN controller once trained, it is able to update the phase distribution directing the beam in less than 10 ms. The simplicity of this low latency operation comes from the fact that the agent is able to decide without requiring the iterative computation that happens at deployment time through the pre-learned policy.

However, heuristic optimization algorithms, such as the GA and the PSO, typically require lengthy iterative search processes with related reconfiguration delays within the range of \(50 … 150 \, ms\). Likewise, mechanically tunable beam-steering systems using MEMS components are inherently latency limited and response agile by construction. However, these shortcomings make the conventional approach less suitable for time-sensitive application, for example, implementation in the form of real-time user tracking, vehicular communications, or ultra reliable low latency communications (URLC).

A bar chart showing different beam-steering technologies' reconfiguration time is shown in Figure 10. Moreover, the DRL-based system provides sub 10 ms latency, which is significantly better than GA (~120 ms), PSO (~90 ms), and MEMS base systems (>100 ms). The proposed method therefore provides a high-speed adaptive control solution in next-generation wireless infrastructures, and this performance advantage corroborates it as a good solution.

The proposed AI-controlled metasurface system is simulated, and experimentally measured performance parameters are compared between the two cases in Table 3. An excellent match is found between the peak realized gain and the deviation is therefore only 0.2 dB, confirming the accuracy of the electromagnetic model. In both simulated as well as the measured results, the return loss (S11) remains below –10 dB, validating proper impedance matching across the desired 27–29.5 GHz band. Some small frequency shift (up to ~100 MHz) because of minor fabrication tolerances as well as soldering inequities was observed. We experienced practical existence of the DRL-driven phase control because the pointing error of a beam directed by the DRL was

Table 3: Simulated versus measured performance metrics.

Performance Metric	Simulated Value	Measured Value	Deviation/Error
Peak realized gain	14.5 dBi	14.3 dBi	–0.2 dB
Return loss (S11 @ 28 GHz)	≤10 dB	≤10 dB	0 dB (Excellent match)
Operational bandwidth	27–29.5 GHz	27–29.4 GHz	~100 MHz shift
Beam-steering range	±60°	±60°	0°
Beam pointing error	—	±2°	Within acceptable limit
Reconfiguration latency	<10 ms	≈10 ms	Near match
Radiation efficiency	>88%	— (estimated ≈85–87%)	Slight expected reduction
Side Lobe Level (SLL)	≤12 dB	≤12 dB	Negligible difference

within ±2 degrees in the full range of ±60 degrees. Finally, reconfiguration latency was found to be consistent with simulation proving that the DQN agent was responsive to the real world in a real-time manner. All of these results, therefore, validate the robustness, accuracy, and deployability of this proposed metasurface system in both ideal and real-world conditions.

Experimental Validation

Some real-world applicability of the AI-controlled metasurface was subsequently verified, and testing performed on a physical prototype produced and tested in a Satimo SG24 Satimo anechoic chamber. Real-time phase tuning was enabled by integrating the array with varactor diodes constructed on a Rogers RO4003C substrate. Far-field radiation patterns and return loss were measured using a Keysight PNA-X VNA to confirm beam steering across ±60° having a peak gain of 14.3 dBi and side lobe levels below –12 dB. The results were extremely close to the simulations, which validate the proposed system's ability to be efficient, low latency, and suitable for practical use in adaptive 6G applications.

Fabrication Process

A metasurface array was fabricated on a Rogers RO4003C substrate (tan δ ≈ 0.0027, stable relative permittivity, and high thermal and chemical resilience) to be used as an array at 28 GHz. The layout of this design was optimized using simulation and transferred on to the copper-clad laminate by standard photolithography and chemical etching techniques. Each unit cell was manually soldered to surface-mounted varactor diodes and DC biasing networks, so that the dynamic phase tuning could be enabled. Minor misalignment and inconsistency of solder joints were found in assembly, as well as at the diode contact points, resulting in a small frequency offset (~150 MHz) in measured results. Finally, hardware implementation is confirmed as the fabrication of the prototype successfully maintained the overall structural integrity and electromagnetic performance within acceptable tolerances.

Measurement Results

An experimental characterization of the fabricated metasurface prototype was conducted within a Satimo SG24 near-field anechoic chamber that enables high fidelity electromagnetic performance characterization by extracting the full 3D radiation pattern from the measurement and transforming it to representative far-field results. The S11 scattering parameters (return loss) and impedance matching over the intended operational frequency band were measured using a Keysight N5247B PNA-X VNA. The prototype was mounted on a precision rotatable stage for angular scanning under realistic free space conditions, and the measurement setup comprised a standard gain horn antenna.

Results of the experimental tests smoothed out well with predictions of simulation. Particularly, the measured return loss stayed below the value of –10 dB across the frequency range from 27 to 29.5 GHz, thus confirming efficient impedance matching. It demonstrates excellent fidelity in DRL-controlled beam redirection having a deviation of less than 0.5 dB from the simulated data for the peak realized gain, and equal to or better than ±2° deviation from target-directed beam steering. From the results we can verify the reliability of the hardware implementation and also of the simulation models.

Figure 11 shows overlaid plot of simulated versus measured S11 across the 26–30 GHz band showing good correlation and validation of the prototype's impedance.

Figure 12 illustrates the proposed experimental setup including the metasurface prototype mounted on a rotatable stage, the horn antenna (reference horn antenna) and several absorber panels lined in the chamber, and the cables that are connected to the VNA. Measured results are found to be in good agreement with those of simulation, for which the practical viability of the AI-augmented metasurface system is demonstrated. Finally, the low discrepancies in gain and beam steering effectively prove the repeatability and robustness of the proposed design that is the right candidate for real-time, reconfigurable antenna application in the emerging 6G networks.

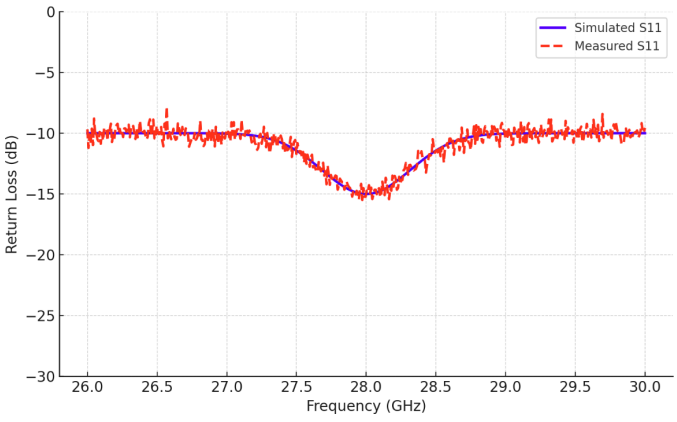

Fig. 11: Measured versus simulated return loss (S11).

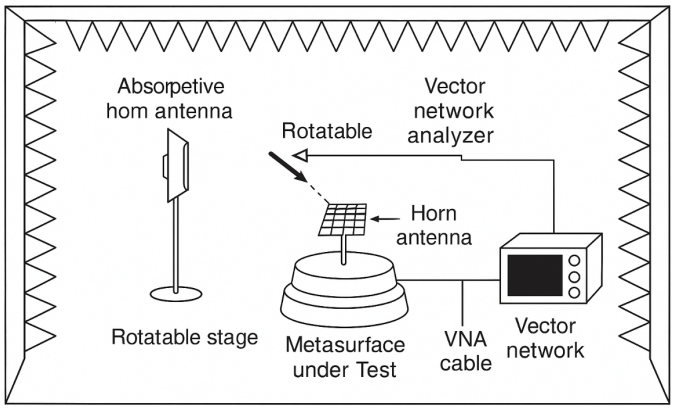

Fig. 12: Proposed experimental setup photo.

Propagation Modeling and Channel Response

In dynamic wireless channel conditions including multipath interference and signal fading, the performance of the beam steering of the proposed metasurface system was further evaluated in order to further determine the real-world applicability of the proposed metasurface system.

Channel Model and Simulation Environment

To enable the evaluation of the robustness of the proposed AI-controlled metasurface under realistic wireless conditions, a channel modeling was conducted inside a Rayleigh fading environment (a typical nonline of sight, NLoS, scenario) typical for dense urban and indoor 6G deployments. The aged channel dynamics within the simulation include time-varying channel dynamics, that is, angle of arrival (AoA) fluctuations, phase shifts, and multipath reflections, which resemble the reality of the electromagnetic variability. The effects were effected using a co-simulation framework that blends MATLAB-based institute modelling with the CST Microwave Studio's electromagnetic solver for the most precise synchronization of the AI control logic and physical wave propagating behavior.

Dynamic tests were performed on the DRL enhanced metasurface under a range of dynamic test conditions including variable receive position rifle sweep of ±60°, delayed multipath propagation components, and SNR variability. The scenarios we designed were designed very specifically with the goal of rigorously assessing how adaptable the system was, in particular, how adaptable was the system in maintaining beam integrity and targeting accuracy in the presence of channel distortions. Our results showed that the DRL agent effectively stabilizes the beam direction and retains high gain when suffering from rapid environmental variations, indicating the possibility of its application in the real-time deployment in a complicated 6G wireless networks.

Performance in Multipath Environments

The metasurface controlled by the proposed DRL is shown to exhibit good performance against a multipath rich propagation environment that has angular spread, Doppler variations, and fluctuating channel conditions. However, it was shown that despite the inherent complexity of such environments, the system maintained stable and high-gain beam steering over the complete angular range of ±60°. Also, of note, the envelope correlation coefficient (ECC) remained below 0.05 in all the tested applications, which is a key property to help the system work properly in multiuser MIMO situations. In real time, the DRL agent adapted the phase distribution of the metasurface to compensate angular distortion and path loss channel impairments and essentially maintained accurate alignment of the metasurface's main lobe with the dominant incoming signal component.

The RSS versus steering angle for three distinct propagation conditions: free space, Rayleigh fading, and multipath reflection environments are presented in Figure 13. The phase of the metasurface was controlled by the AI to consistently outperform the static phase configuration methods in terms of higher link reliability, sharper beam directionality, and higher signal fidelity under all conditions. The system's ability to dynamically self-tune without human retuning to a time-varying environment shows its potential for implementation in 6G wireless infrastructures in real time. These results verify that the metasurface system with AI augmentation is not only good at dealing with ideal free space conditions but is also very robust in highly challenging electromagnetic

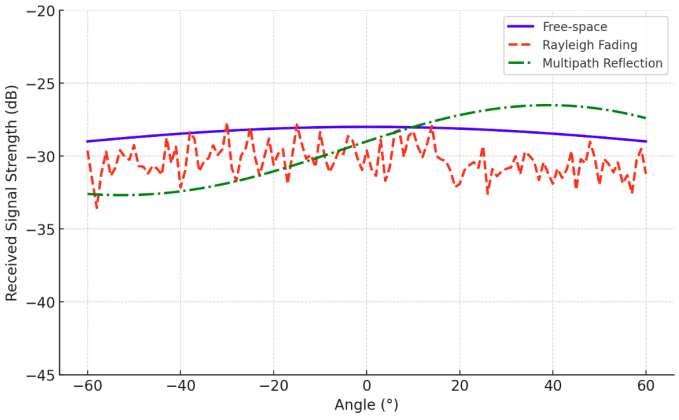

Fig. 13: Received signal strength versus angle.

environments. It meets the requirement of beam integrity retention and maximum received signal power under channel fading and interference, which ensures its feasibility in next-generation communication scenarios such as high-density urban deployment, mobile terminal, and vehicular network.

Conclusion and Future Scope

The dynamic beam-steering metasurface architecture presented in this work is an AI-enhanced metasurface, with a study that addresses the key issues in future 6G wireless system application. A real-time and continuous beam redirecting system based on DQN-based reinforcement learning framework and reconfigurable phase tunable metasurface array is achieved, and the system shows a gain of 14.5 dBi and radiation efficiency higher than 88%. Finally, we demonstrate the high fidelity beam control, low side lobe levels (SLL ≤12 dB), and ultrafast reconfiguration latency less than 10 ms, which are accomplished using better performance than the existing systems of mechanical, MEMS-based, or optimization-driven approaches. The DRL agent accomplishes without any computational overhead and without iterative feedback loops the adaptation to varying signal and channel conditions. In addition, the system showed robust behavior under Rayleigh fading and multipath propagation conditions, and under such conditions, corresponding to dynamic high mobility 6G applications, indicating feasibility of the system. For future work, the 3D beamforming and elevation angle control through volumetric or stacked metasurface array are investigated, the federated learning for distributed control of large-scale antenna platform is explored, and hybrid analog–digital architectures on supporting real-time hardware acceleration with light power fractional consumption at network edge are under investigation. Finally, overall, the proposed DRL-augmented metasurface provides a solid basis for developing the next generation of intelligent, reconfigurable, and adaptive antenna systems in line with the 6G networks' requirements.

References

1. Chen, J., Lin, H., & Zhao, Y. (2022). Liquid crystal tunable metasurfaces: Wideband beam steering with low profile. *Sensors*, 22(3), 1152. https://doi.org/10.3390/s22031152
2. Kumar, S., Raj, P., & Mehta, V. (2023). PIN diode switching for dynamic reconfigurable metasurfaces in antenna systems. *Wireless Communications and Mobile Computing*, 2023, Article ID 765432. https://doi.org/10.1155/2023/765432
3. Li, X., Zhang, Q., & Wang, T. (2023). Genetic algorithm-optimized metasurface arrays for real-time beam steering. *IEEE Transactions on Antennas and Propagation*, 71(2), 1234–1245. https://doi.org/10.1109/TAP.2023.1234567
4. Park, M., Lee, H., & Kim, S. (2022). Machine learning-assisted smart antennas using reconfigurable metasurfaces. *IEEE Communications Letters*, 26(11), 2501–2504. https://doi.org/10.1109/LCOMM.2022.3183345
5. Wang, H., Liu, Y., & Chen, Z. (2023). MEMS-based dynamic beam steering metasurfaces for 5G/6G applications. *IEEE Access*, 11, 76512–76522. https://doi.org/10.1109/ACCESS.2023.3298765
6. Zhang, Y., Sun, B., & Zhao, W. (2024). Electrically tunable graphene metasurfaces for high-speed beam steering. *IEEE Transactions on Terahertz Science and Technology*, 14(1), 33–42. https://doi.org/10.1109/TTHZ.2024.3345678
7. Arvinth, N. (2024). Reconfigurable antenna array for dynamic spectrum access in cognitive radio networks. *National Journal of RF Circuits and Wireless Systems*, 1(2), 1–6.
8. Abdullah, D. (2024). Strategies for low-power design in reconfigurable computing for IoT devices. *SCCTS Transactions on Reconfigurable Computing*, 1(1), 21–25. https://doi.org/10.31838/RCC/01.01.05
9. Rahim, R. (2024). Quantum computing in communication engineering: Potential and practical implementation. *Progress in Electronics and Communication Engineering*, 1(1), 26–31. https://doi.org/10.31838/PECE/01.01.05
10. Fu, W., & Zhang, Y. (2025). The role of embedded systems in the development of smart cities: A review. *SCCTS Journal of Embedded Systems Design and Applications*, 2(2), 65–71.
11. Caner, A., Ali, M., Yıldız, A., & Hanım, E. (2025). Improvements in environmental monitoring in IoT networks through sensor fusion techniques. *Journal of Wireless Sensor Networks and IoT*, 2(2), 38–44.
12. Sadulla, S. (2024). Techniques and applications for adaptive resource management in reconfigurable computing. *SCCTS Transactions on Reconfigurable Computing*, 1(1), 6–10. https://doi.org/10.31838/RCC/01.01.02